

## Asymmetric spin transitions of nonthermalized $\text{Mn}^{2+}$ ions in $(\text{Zn},\text{Mn})\text{Se}$ -based quantum wells

D. Kudlacik,<sup>1</sup> K. V. Kavokin,<sup>2</sup> C. Lüders,<sup>1</sup> K. Barthelmi,<sup>1</sup> J. J. Schindler<sup>Ⓞ</sup>,<sup>1</sup> H. Moldenhauer<sup>Ⓞ</sup>,<sup>1</sup> P. Waldkirch,<sup>1</sup> V. F. Sapega,<sup>3</sup>  
D. R. Yakovlev,<sup>1,3</sup> A. Waag,<sup>4</sup> M. Bayer,<sup>1,3</sup> and J. Debus<sup>Ⓞ</sup>,<sup>1,\*</sup>

<sup>1</sup>*Experimentelle Physik 2, Technische Universität Dortmund, 44227 Dortmund, Germany*

<sup>2</sup>*Spin Optics Laboratory, Saint-Petersburg State University, 198504 St. Petersburg, Russia*

<sup>3</sup>*Ioffe Institute, Russian Academy of Sciences, 194021 St. Petersburg, Russia*

<sup>4</sup>*Institute of Semiconductor Technology, University of Braunschweig, 38106 Braunschweig, Germany*



(Received 13 May 2019; revised manuscript received 10 February 2020; accepted 2 April 2020; published 30 April 2020)

In  $\text{Zn}_{1-x}\text{Mn}_x\text{Se}/(\text{Zn},\text{Be})\text{Se}$  quantum wells with  $x < 0.035$ , nonthermalized  $\text{Mn}^{2+}$  ions demonstrate in spin-flip scattering spectra multiple Stokes and anti-Stokes transitions whose absolute energies deviate by up to 20% from each other. This asymmetry is tuned significantly by the optical power density, magnetic field direction, and Mn ion concentration. The nonequidistant  $\text{Mn}^{2+}$  spin transitions are modeled by the Zeeman splitting and quadrupolar crystal-field components taking values of up to 7 GHz. We suggest that nonequilibrium carriers dynamically polarize the Mn-ion spins so that they occupy levels with positive and negative spin projection numbers giving rise to asymmetric spin transitions.

DOI: [10.1103/PhysRevB.101.155432](https://doi.org/10.1103/PhysRevB.101.155432)

Magnetic semiconductors offer great potential for efficient spin injection and magnetization manipulation by electrical and optical methods and demonstrate promising spin-processing functionalities with regard to collective spin ordering phenomena [1,2]. The magnetic ions, predominantly manganese ions embedded in II-VI or III-V semiconductors that possess a total electron spin of  $s = 5/2$ , have unique properties showing giant magneto-optical effects and microsecond spin lifetimes, which make them attractive to optical manipulation [3–8]. Recently, a vivid research on optical properties of  $\text{Mn}^{2+}$  ions in perovskite nanocrystals has started [9–11]. For developing optical manipulation protocols, it is highly crucial to identify and tailor the interactions between the spins of the  $\text{Mn}^{2+}$  ions and carriers. In that context, peculiarities in the spin splitting of the  $\text{Mn}^{2+}$  ions which defines their Larmor spin precession have been observed; in II-Mn-VI structures with selenides or sulfides and Mn concentrations above the percolation threshold of 18%, effective internal fields lead to shifts in their electron-paramagnetic resonance fields mainly due to the Dzyaloshinsky-Moriya interaction between  $\text{Mn}^{2+}$  ions [12]. In  $(\text{Cd},\text{Mn})\text{Te}$ -based quantum wells, the  $\text{Mn}^{2+}$   $g$  factor is changed by the interaction with photogenerated holes [13], and in a bulk  $(\text{Cd},\text{Mn})\text{Te}$  crystal the effect of the local crystal field is suppressed at specific magnetic field orientations [3].

We report on energetically asymmetric spin transitions of nonthermalized  $\text{Mn}^{2+}$  ions for resonant exciton excitation in  $\text{Zn}_{1-x}\text{Mn}_x\text{Se}/(\text{Zn},\text{Be})\text{Se}$  quantum wells (QWs) with  $x < 0.035$  using the spin-flip Raman scattering technique. The Stokes and anti-Stokes spin transitions differ in energy by up to 113  $\mu\text{eV}$  from each other. The difference is enhanced by an intense photoexcitation and at magnetic field directions

slightly tilted from the QW growth axis. For weak laser power densities or considerably oblique magnetic fields, the spin transitions become symmetric and equal to the Zeeman splitting expected for  $\text{Mn}^{2+}$  ions with an isotropic  $g$  factor of 2.0. We theoretically describe the asymmetry in the spin-transition energies by the quadrupolar component of the crystal field at the Mn ion sites taking values of 7 GHz. Comparison to simulation provides evidence that nonthermalized Mn ions with negative spin quantum numbers  $m_s$  are necessary to allow for observing anti-Stokes spin scattering and, in turn, the asymmetry in the spin-transition energies. Our results are relevant to photoexcited systems with spin  $s > 1/2$  in low-symmetric crystal fields or in presence of strong anisotropic exchange interaction, and may be used to manipulate spin-transition energies of transition metal ions in semiconductor nanostructures for optical and magnetic resonance experiments.

We studied  $\text{Zn}_{1-x}\text{Mn}_x\text{Se}/\text{Zn}_{0.94}\text{Be}_{0.06}\text{Se}$  QW structures with  $x = 0.004, 0.012, 0.020,$  and  $0.035$  and type-I band alignment. The nominally undoped samples were grown by molecular-beam epitaxy on (001)-oriented GaAs substrates. Unless specified otherwise, results for the QW with  $x = 0.012$  are shown in the following. The samples were mounted strain free inside a magnet cryostat, which provided magnetic fields up to 10 T. The temperature was set to 1.6 K. The 10-nm-thick QWs were excited by the second harmonic of a tunable continuous-wave Ti:sapphire laser with intracavity frequency doubling. The laser power was stabilized by a liquid-crystal variable attenuator and the power density was usually about  $5 \text{ W}/\text{cm}^2$  at the sample surface. Each sample was covered by a mask having a hole of 300- $\mu\text{m}$  diameter; typically, the central part of  $50 \times 50 \mu\text{m}^2$  size of the fully illuminated accessible sample area was selected for the detection by a cross slit. The QW emission was spectrally resolved by a double monochromator equipped with a Peltier-cooled GaAs photomultiplier

\*Corresponding author: joerg.debus@tu-dortmund.de

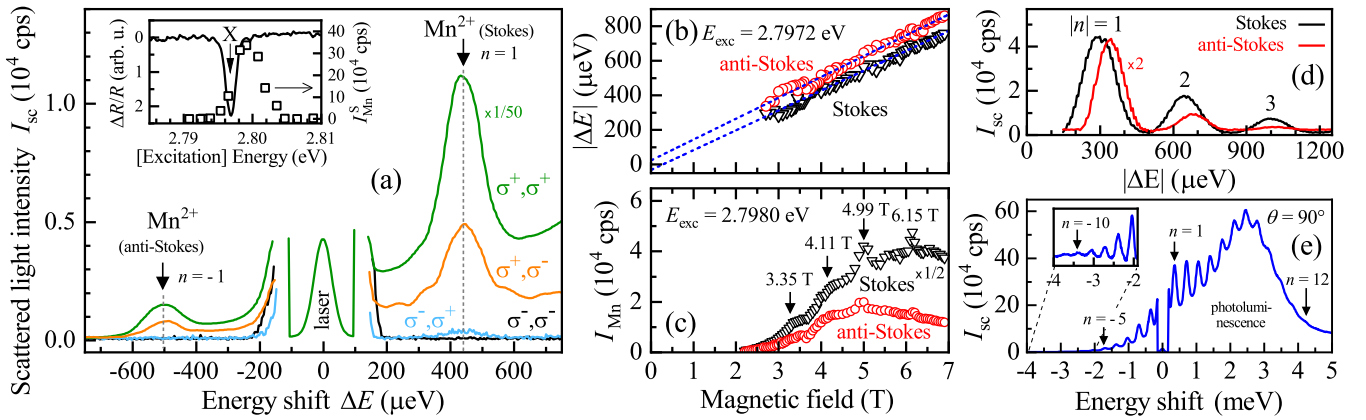


FIG. 1. (a)  $\text{Mn}^{2+}$  spin scattering spectra for circularly cross- and copolarized configurations;  $E_{\text{exc}} = 2.7980$  eV. (Inset) White-light reflectivity contrast spectrum with the resonance of the bright exciton (solid line) and the  $n = 1$   $\text{Mn}^{2+}$  spin-scattering resonance profile (squares). Magnetic field dependence of the (b) absolute energy shifts and (c) scattering intensities of the  $|n| = 1$   $\text{Mn}^{2+}$  resonances. (d) Spectra of high-order S and AS  $\text{Mn}^{2+}$  resonances. (e) In Voigt geometry up to ten clear  $\text{Mn}^{2+}$  resonances (see inset,  $I_{\text{sc}}$ -axis rescaled) are observed in the anti-Stokes regime;  $B = 2.9$  T and  $E_{\text{exc}} = 2.8164$  eV.

[14,15]. The backscattering experiments were performed in Faraday geometry ( $\theta = 0^\circ$ ) and in tilted geometries, where the magnetic field  $\mathbf{B}$  and QW growth axis  $\mathbf{z}$  enclosed an angle of  $\theta$  within the  $yz$  plane. The circular polarization of light is denoted by  $\sigma^\pm$ , where the signs  $\pm$  are determined by the sign of the photon angular momentum projection on the optical  $z$  axis [16]. The spectra were merely measured in the  $(\sigma^+, \sigma^+)$  polarization configuration.

In Faraday geometry, see Fig. 1(a), the spin scattering of  $\text{Mn}^{2+}$  is observed at the Stokes (S) and anti-Stokes (AS) side, for  $\sigma^+$  polarized excitation of the QW exciton (X) with total angular momentum of  $+1$ , as shown in the inset of Fig. 1(a). The energies of the first-order ( $|n| = 1$ ) spin resonances are  $\Delta E_S = (437 \pm 5) \mu\text{eV}$  and  $\Delta E_{AS} = (-505 \pm 5) \mu\text{eV}$  measured at 4 T. Remarkably, they differ by  $\delta E = |\Delta E_{AS}| - |\Delta E_S| = 68 \mu\text{eV}$  from each other. Describing the  $\text{Mn}^{2+}$  spin splitting in terms of a  $g$  factor, we obtain  $g_{\text{Mn}} = 1.887$  (2.181) for Stokes (anti-Stokes) scattering. Both values deviate significantly from the isotropic  $\text{Mn}^{2+}$   $g$  factor of 2.0 [12,17,18]. Moreover, the  $\text{Mn}^{2+}$  spin scattering appears predominantly at  $\sigma^+$  polarized excitation. It is consistent with both the signs of the electron and heavy-hole exchange constants as well as the magnitude of the giant Zeeman splitting of the exciton states [19,20]. For the QW with  $x = 0.012$ , the exciton Zeeman splitting is given by about 38 meV at 4 T which reduces drastically the probability of state mixing giving rise to strict polarization selection rules [21].

For increasing the magnetic field strength from 4 to 7 T, the difference between the S and AS spin scattering energies remains practically unchanged, as shown in Fig. 1(b). Linear fits of the magnetic field evolutions of  $|\Delta E|$  yield  $\delta E \approx 61 \mu\text{eV}$ , see the blue dashed lines [22]. It is worthwhile to outline that the asymmetry in the energies is not only limited to the first-order  $\text{Mn}^{2+}$  spin resonance; also high-order resonances exhibit a pronounced  $\delta E$ , as depicted in Fig. 1(d) for  $|n| \leq 3$ . Here, the Stokes and anti-Stokes lines differ by a constant  $\delta E$  from each other. Differences are also observed in the intensities  $I_{\text{Mn}}$  of the  $\text{Mn}^{2+}$  spin resonances. While the Stokes

line is at least two times larger than the respective anti-Stokes line, as is shown in Figs. 1(a) and 1(d), the magnetic field dependence of  $I_{\text{Mn}}$ , see Fig. 1(c), indicates that the S scattering is more strongly enhanced than the AS process with increasing magnetic field strength, in particular, due to the decrease of  $I_{\text{Mn}}^{\text{AS}}$  for  $B > 5$  T.

A clear interdependence between the intensity ratio and  $\delta E$  is outlined by tuning  $\delta E$  through the optical excitation density, as depicted in Fig. 2(a). Increasing the laser power density

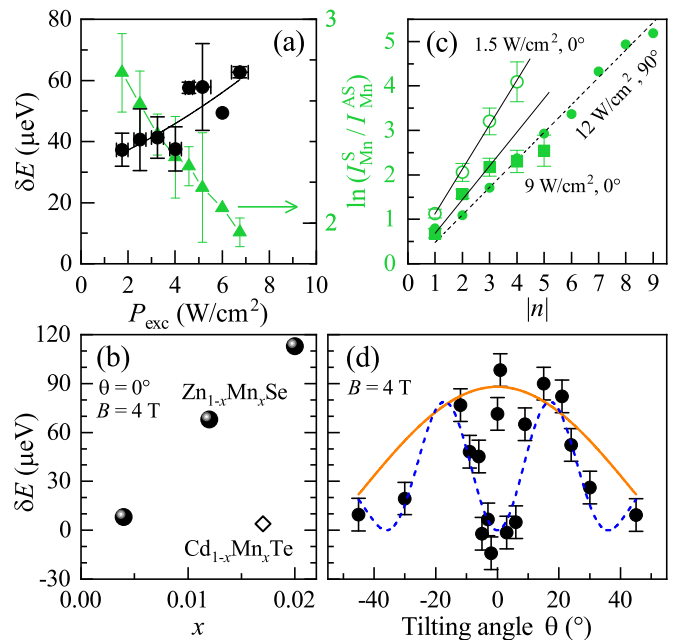


FIG. 2. (a) Dependence of  $\delta E$  on the laser power density; 100  $\mu\text{m}$  width of the intermediate cross slit,  $B = 4$  T. Natural logarithm of the ratio of the S and AS spin scattering intensities as a function of (a)  $P_{\text{exc}}$ , see right scale, and (c) the absolute  $\text{Mn}^{2+}$  resonance number for different  $P_{\text{exc}}$ ; lines are guides for the eye. Dependence of  $\delta E$  on the (b) Mn ion concentration and (d) tilting angle  $\theta$ ; fit results on basis of Eq. (2) are shown by the curves.

$P_{\text{exc}}$  enhances the Stokes/anti-Stokes energy asymmetry and, in turn, decreases the natural logarithm of  $I_{\text{Mn}}^{\text{S}}/I_{\text{Mn}}^{\text{AS}}$ .  $\delta E$  can further be changed by selecting specific laser illuminated sample areas; the central part of the laser spot with a high average laser power yields larger  $\delta E$  values compared to the spatially outer parts of the Gaussian shaped laser spot.

The asymmetry in the spin-transition energies is a feature of the (Zn,Mn)Se-based QWs. By comparison, in (Cd,Mn)Te-based QWs  $\delta E$  vanishes, for exciting the exciton, irrespective of the laser power applied. In a 20-nm-thick Cd<sub>0.983</sub>Mn<sub>0.017</sub>Te/(Cd,Mg)Te QW  $\delta E$  amounts to  $-4 \mu\text{eV}$  [Fig. 2(b)]. Changing the Mn ion concentration may enhance the asymmetry in the energies. For the Zn<sub>0.996</sub>Mn<sub>0.004</sub>Se QW,  $\delta E = (-8 \pm 6) \mu\text{eV}$  is also negligibly small, while the sample with  $x = 0.020$  demonstrates a  $\delta E$  of  $(-113 \pm 6) \mu\text{eV}$ . A further increase in the Mn ion concentration, as in the case of the Zn<sub>0.965</sub>Mn<sub>0.035</sub>Se QW, results in a considerable broadening of the S and AS lines, which prevents from determining an asymmetry in the energies. The broadening is most probably due to enhanced Mn-Mn spin interactions which also manifest themselves in short Mn-spin coherence times being characteristic for high Mn-ion doping levels [23].

A further set screw of the spin scattering asymmetry is provided by the magnetic field direction; the dependence of  $\delta E$  on the tilting angle  $\theta$  is shown for  $B = 4 \text{ T}$  in Fig. 2(d). For large tilting angles  $|\theta| > 10^\circ$ ,  $\delta E$  decreases to small values. Of particular interest is the behavior around the Faraday geometry: For  $|\theta| < 15^\circ$ ,  $\delta E$  demonstrates a W-shaped behavior symmetric to  $0^\circ$ . The angular dependence is a key aspect in finding the mechanism of the asymmetric Mn<sup>2+</sup> spin scattering, as will be discussed in the following.

The multiple Mn<sup>2+</sup> spin scattering is realized through anisotropic exchange interaction between the photoexcited heavy-hole and a number of Mn<sup>2+</sup> ions, which form a hole magnetic polaron [24–27]. For Stokes (anti-Stokes) scattering, the exciton energy is reduced (increased) by changing the spin of an Mn ion to a higher (lower) lying level. While Stokes scattering predominantly occurs between levels with initial  $m_s > 0$ , anti-Stokes scattering requires a finite occupation of Mn<sup>2+</sup> spin levels with negative  $m_s$ . These Mn ions, which are not thermalized to the lowest spin levels with positive  $m_s$ , are present due to exchange scattering with photoexcited carriers which do not have a maximum spin projection on the exchange field. When these carriers relax through flip-flop transitions involving some Mn spins to their spin ground state, they turn the magnetic moments of these Mn spins opposite to the external magnetic field. The nonthermalized Mn ions have different spin orientations with respect to  $\mathbf{B}$ . A similar effect of the formation of hot spin domains was observed by Teppe *et al.* [28] and was theoretically analyzed by Kavokin and Malpuech [29].

The  $3d$  electron levels of an Mn<sup>2+</sup> ion are split not only by the Zeeman energy,  $E_Z = \mu_{\text{B}}g_{\text{Mn}}B$  with the Bohr magneton  $\mu_{\text{B}}$ , but also by the crystal field (CF) at the Mn site. A QW with symmetric confinement potential has the point symmetry  $D_{2d}$  [30]. In presence of in-plane strain or a magnetic field, the symmetry is reduced and, therefore, the quadrupole contribution of the electric field from the host crystal ions is taken into account at the Mn<sup>2+</sup> ion site. For such a CF gradient, the

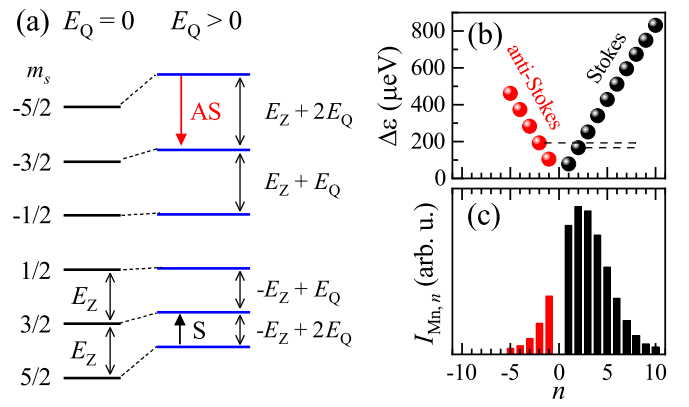


FIG. 3. (a) Mn<sup>2+</sup> spin levels and exemplary spin transitions for  $E_Q = 0$  and  $E_Q > 0$ ;  $B > 0$ . Energy differences are indicated by double-sided arrows. (b) Crystal-field correction to the Zeeman energy and (c) scattering intensity as function of  $n$  calculated for  $B = 7.5 \text{ T}$ ,  $E_Q = 60 \mu\text{eV}$ ,  $\theta = 30^\circ$ , and  $T_{\text{Mn}} = 11.5 \text{ K}$ .

Hamiltonian of the electric quadrupole interaction reads [31]

$$H_Q = \frac{E_Q}{4} \left[ m_s^2 - \frac{\hat{I}(\hat{I} + 1)}{3} \right] [3 \cos^2 \varphi - 1 - \eta \sin^2 \varphi \cos(2\phi)]. \quad (1)$$

Here,  $E_Q$  is the quadrupole splitting energy,  $\hat{I}$  the quadrupole tensor operator,  $0 \leq \eta \leq 1$  accounts for the CF symmetry, and the polar angle between  $\mathbf{B}$  and the quadrupole axis is given by  $\varphi$  which approximately coincides with  $\theta$ . The angle  $\phi$  ranges from  $0^\circ$  ( $x$  axis) to  $90^\circ$  ( $y$  axis). The impact of the CF on the  $3d$  level splitting and spin transitions is sketched, for Faraday geometry, in Fig. 3(a). The different shifts in the energies of the spin levels result from the quadrupole interaction term. The Mn<sup>2+</sup> Stokes spin transition is smaller than the Zeeman energy, while the anti-Stokes spin transition is increased by  $E_Q$  or  $2E_Q$  with respect to  $E_Z$ . The experimental data demonstrate that the energy of the AS spin transition typically exceeds that of the Stokes transition. It indicates that the AS (S) scattering is predominantly performed from spin levels with negative (positive)  $m_s$  including transitions from spin levels with  $|m_s| = 3/2$  and  $5/2$ . On basis of the Zeeman and CF terms, the energy difference between anti-Stokes and Stokes transitions is given by

$$\delta E = E_Q(|m_s| - 1/2)[3 \cos^2 \theta - 1 - \eta \sin^2 \theta \cos(2\phi)]. \quad (2)$$

This equation accounts for, in particular, the angular dependence of the asymmetry in the spin transitions. It merely depends on the initial Mn spin orientation  $m_s$  and the magnetic field geometry.

Fitting Eq. (2) with  $|m_s| = 5/2$ ,  $\phi = 0^\circ$  and  $\eta = 0$  to the experimentally obtained angle dependence of  $\delta E$  yields the orange curve presented in Fig. 2(d). The  $E_Q$  value amounts to about  $30 \mu\text{eV}$  (7 GHz). By increasing the asymmetry factor to  $\eta = 0.7$  and weighting the transitions from  $|m_s| = 5/2$  with respect to that from  $|m_s| = 1/2$  in the proportion 10 : 1, the blue curve results from the fitting. However, the points measured at the Faraday geometry ( $\pm 1^\circ$ ) significantly deviate from Eq. (2). The agreement of the fitting curve with the data points at the Faraday geometry may be enhanced by including high-order crystal-field terms, see p. 236 in Ref. [31]. Such

an inclusion would attach additional importance to  $\eta$  and, in particular, to the field gradient  $q$ , see [32], which appears in the high-order components. A further ingredient of the  $\delta(\theta)$  dependence may also be the dynamic polarization of the  $\text{Mn}^{2+}$  ions and, in turn, the transition probabilities between the different  $\text{Mn}^{2+}$  spin levels in dependence on the magnetic field direction. Both the explicit value of  $q$  as well as an extension of  $\delta(\theta)$  by the transition probabilities fall outside of the scope of our current study.

In order to describe the asymmetric spin transitions for a nonthermalized Mn spin system, we now evaluate the probability of spin transitions for a single Mn ion and the statistical distribution of the number of spin transitions in the Mn-ion ensemble; both positive as well as negative spin projection numbers are included. The transition probability between, for example, the levels  $|m_s\rangle$  and  $|m_s + 1\rangle$  of a certain Mn spin is given by perturbation theory to

$$W_{m_s, m_s+1} = W_{m_s+1, m_s} = \langle m_s + 1 | M_y | m_s \rangle^2 b_y^2 \tau / \hbar^2,$$

where  $M_y$  is the  $\text{Mn}^{2+}$  magnetic moment projection on the  $y$  axis perpendicular to  $\mathbf{B}$ ,  $b_y$  is the  $y$  projection of the exchange field,  $\tau$  is the spin scattering time. In an ensemble of  $N$  Mn spins, the average number of transitions between levels with  $m_s$  and  $m_s + 1$  is described by  $p_{S, m_s} = N \rho_{m_s} W_{m_s+1, m_s}$  and  $p_{AS, m_s} = N \rho_{m_s+1} W_{m_s, m_s+1}$ , where  $\rho_{m_s}$  and  $\rho_{m_s+1}$  are the probabilities to find an Mn ion in a respective spin state. For a thermalized Mn spin system, the S and AS average transition numbers differ in the Boltzmann factor. Random numbers of transitions to low- and high-lying levels,  $n_S$  and  $n_{AS}$ , obey the Poisson distribution:

$$P(n_{S, m_s}) = \frac{p_{S, m_s}^{n_{S, m_s}}}{n_{S, m_s}!} \exp(-p_{S, m_s}), \quad (3)$$

$$P(n_{AS, m_s}) = \frac{p_{AS, m_s}^{n_{AS, m_s}}}{n_{AS, m_s}!} \exp(-p_{AS, m_s}).$$

The distribution of the total number  $L_{m_s}$  of Zeeman energy quanta  $E_{Z, m_s}$  in a multi-spin-flip scattering spectrum is obtained from Eq. (3) by averaging over all possible S and AS transitions:

$$P_{m_s}(L_{m_s}) = \left( \frac{p_{S, m_s}}{p_{AS, m_s}} \right)^{\frac{L_{m_s}}{2}} \sum_{K=0}^{\infty} \frac{(p_{S, m_s} p_{AS, m_s})^{\frac{|L_{m_s}|}{2+K}}}{(|L_{m_s}| + K)! K!} e^{-\gamma} \quad (4)$$

with  $\gamma = p_{S, m_s} + p_{AS, m_s}$ . A multi-spin-flip scattering spectrum is formed by superimposing series of lines corresponding to different pairs of spin levels ( $m_s, m_s + 1$ ). Since these series of lines have different energies, the peaks in a multi-spin-flip scattering spectrum will be broadened and may be shifted towards lower or higher energy. In the following, we suppose that transitions corresponding to different  $m_s$  are not resolved due to spectral line broadening. We calculate the deviation of the mean energy position from the Zeeman resonance, for the  $n$ -th peak in the multi-spin-flip scattering sequence, and the total intensity of the  $n$ -th peak:

$$\Delta \varepsilon_n = I_{\text{Mn}, n}^{-1} \left[ \sum_{\Delta L} \prod_{m_s} P_{m_s}(L_{m_s}) \delta' \sum_{m_s} L_{m_s} E_{Z, m_s} \right], \quad (5)$$

$$I_{\text{Mn}, n} = \sum_{\Delta L} \prod_{m_s} P_{m_s}(L_{m_s}) \delta' \quad (6)$$

with  $\delta' = \delta_{n - \sum_{m_s} L_{m_s}}$  and  $\Delta L = L_{-s}, \dots, L_s$ . For a nonthermalized Mn spin system with an effective spin temperature of 11.5 K,  $\Delta \varepsilon_n$  exhibits an asymmetry, marked by the dashed lines for negative and positive  $n$  in Fig. 3(b). This is possible due to the finite occupation of Mn levels with negative  $m_s$ . This level occupation is tunable through the laser power density which is coupled to the number of photoexcited carriers. They, in turn, change through spin flip-flop processes the spin orientations of the  $\text{Mn}^{2+}$  ions with respect to the external magnetic field. Moreover, the calculation yields five AS lines which further underlines the nonthermalized state of the Mn spin system, as shown in Fig. 3(c).

The appearance of AS lines as well as the intensity ratio between the Stokes and anti-Stokes scattering lines are relevant to decide on the thermalization state of the Mn spin system. For thermalized Mn ions with a spin temperature  $T_{\text{Mn}}$ , the difference between the S and AS average transition numbers is determined by the Boltzmann factor  $\exp(\mu_B g_{\text{Mn}} B / k_B T_{\text{Mn}})$ . The logarithm of the ratio between the S and AS peak intensities with the same number  $n$  is then given by

$$\ln(I_{\text{Mn}}^S / I_{\text{Mn}}^{\text{AS}}) = n \mu_B g_{\text{Mn}} B / (k_B T_{\text{Mn}}). \quad (7)$$

Thus, the dependence of the logarithm of the intensity ratio on  $n$  is linear only for thermalized Mn ions with  $m_s = 5/2$ . For a high laser power density in Faraday geometry, see solid squares in Fig. 2(c),  $\ln(I_{\text{Mn}}^S / I_{\text{Mn}}^{\text{AS}})$  deviates from a linear dependence; hence, it indicates the presence of nonthermalized Mn ions. In that case, the intensity ratio is small, as the AS line becomes more intense than the S line. In Voigt geometry ( $\theta = 90^\circ$ ), the intensity ratio follows a linear dependence. At such large tilting angles, the Mn spin level splitting is determined by the Zeeman term predominantly giving rise to energetically equidistant Mn spin levels; therefore, the asymmetry is negligibly small.

A further evidence for the presence of nonthermalized Mn ions is provided by the appearance of the intensity enhancements at specific magnetic fields [Fig. 1(c)]. This results from the mixing of spin states of single  $\text{Mn}^{2+}$  ions and nearest-neighbor Mn ions, which are antiferromagnetically coupled to pair clusters [21]. One may claim – in contrast to previous publications [24,26] – that Mn pairs contribute to the multiple spin scattering of single  $\text{Mn}^{2+}$  ions. Electrons can inelastically scatter at Mn pairs [33], when the pair axis is not parallel to the QW plane; hence, the squared wave function of a quantum-confined electron is different at the two Mn ions. In contrast to the low-magnetic-field scenario considered in Ref. [33], the giant Zeeman splitting – in our case – will prevent the spin-flip scattering of electrons. As a result, the projection of the total spin of the pair on the magnetic field is conserved. If we further neglect scattering processes to high-excited states, which is correct for intermediate electron temperatures, the electron-induced transitions will couple the states  $s_p = 0$  and the excited triplet  $s_p = 1$  with  $m_{s_p} = 0$  of the Mn pair, where  $s_p$  and  $m_{s_p}$  are the quantum numbers of the pair total spin and its projection on the magnetic field, respectively.

One may think of two possible scenarios within the excited triplet states with  $s_p = 1$ . (i) The Mn pairs are heated up by excitons, and resident electrons provide their cooling to the lattice temperature. Accordingly, the triplet state with  $m_{s_p} = 0$  of the Mn pair becomes less populated than the

states with  $m_{s_p} = \pm 1$ . (ii) Under optical excitation electrons are strongly excited, so that their kinetic temperature exceeds the lattice temperature. If one assumes that the scattering of excitons at pairs is less effective than that of electrons, the triplet state ( $m_{s_p} = 0$ ) becomes more populated than that with  $m_{s_p} = \pm 1$ . In the first case, the Stokes transitions within the excited triplet states of the Mn pair go predominantly from  $m_{s_p} = -1$  to 0, while the anti-Stokes transitions go from  $m_{s_p} = +1$  to 0. In the case (ii), the Stokes processes within the excited triplet are performed in particular from the states  $m_{s_p} = 0$  to  $-1$ , and the anti-Stokes scattering is described by the transition ( $s_p = 1, m_{s_p} = 0$ )  $\rightarrow$  ( $s_p = 1, m_{s_p} = +1$ ). For both cases in consideration of a crystal-field splitting given by Eq. (2), the Stokes and anti-Stokes transitions differ in energy. The sign of the difference will be opposite for cases (i) and (ii). Since the axes of the Mn ion pairs involved in the scattering should not be parallel to the QW plane, the quadrupole crystal-field splitting may in fact originate from anisotropic spin-spin interactions within the pair which split the states with  $m_{s_p} = 0$  and  $m_{s_p} = \pm 1$  of the excited  $s_p = 1$  triplet. Such a scattering of excitons or electrons at Mn pairs may lead to a population difference of states with positive and negative pair-spin quantum numbers. This together with the coupling between single and paired Mn ions may explain the increase of  $\delta E$  observed for increasing Mn ion concentration.

An alternative idea to explain the asymmetric Mn<sup>2+</sup> spin transitions is less probable: The nonlinear energy dispersion of the hole-magnetic polaron or that of an Mn spin wave may give rise to different energies in S and AS scattering processes by analogy with the Brillouin scattering of exciton-polaritons in bulk crystals [34,35]. However,  $k$ -vector dependent scattering experiments could not verify these assumptions.

As described within the frame of Fig. 2(b), a highly excited Mn spin system and thus a spin-transition asymmetry is observed in (Zn,Mn)Se-based QWs, but not in (Cd,Mn)Te

QWs. We propose that the spin-lattice relaxation, which is faster in (Cd,Mn)Te than in (Zn,Mn)Se [36], is one of the key aspects for this observation. In (Cd,Mn)Te, the Mn ions become thermalized more effectively due to a strong coupling to the phonon bath so that the occupation of Mn spin levels with negative  $m_s$  is less probable. Moreover, in weakly strained low-dimensional (Cd,Mn)Te structures a magnetic anisotropy is negligible [37]. This also excludes an asymmetry in the spin transitions for the (Cd,Mn)Te QWs studied. For the (Zn,Mn)Se QWs, as mentioned within the context of Eq. (1), we propose a low symmetry and, in turn, the presence of biaxial (and compressive) strain. Accordingly, the crystal-field amplitude as well as the quadrupole component of the electric field at the Mn ion site become significant [38], probably exceed those in weakly strained (Cd,Mn)Te QWs, and lead to large  $\delta E$  values.

In conclusion, we have found that, for Mn<sup>2+</sup> ions, which are nonthermalized due to exchange scattering with photoexcited carriers, the low-symmetric CF leads to highly different Stokes and anti-Stokes spin scattering energies. Due to the laser-power and magnetic-field tunability the asymmetric spin transitions provide a versatile possibility to meet the resonance conditions of magnetic and optical experiments. The asymmetry in the spin transitions may also provide an optically tunable alternative to strain-induced magnetic anisotropy and, as fine structure affects spin dynamics, it may control the relaxation of spins of transition metal ions in semiconductor nanostructures. In addition to advancing the fundamental understanding of spin scattering of magnetic ions, these results will prove crucial in applications of systems with strong magnetocrystalline effects.

We acknowledge financial support by the DFG and RFBR in the frame of the ICRC TRR 160 (Projects A6, B2, and B4). K.V.K. acknowledges a partial financial support by the St. Petersburg State University (Project No. 40.65.62.2017).

- 
- [1] T. Dietl and H. Ohno, Dilute ferromagnetic semiconductors: Physics and spintronic structures, *Rev. Mod. Phys.* **86**, 187 (2014).
  - [2] *Introduction to the Physics of Diluted Magnetic Semiconductors*, edited by J. Kossut and J. A. Gaj (Springer, Heidelberg, 2010).
  - [3] S. Cronenberger, M. Vladimirova, S. V. Andreev, M. B. Lifshits, and D. Scalbert, Optical Pump-Probe Detection of Manganese Hyperfine Beats in (Cd, Mn)Te Crystals, *Phys. Rev. Lett.* **110**, 077403 (2013).
  - [4] F. Ungar, M. Cygorek, and V. M. Axt, Quantum kinetic equations for the ultrafast spin dynamics of excitons in diluted magnetic semiconductor quantum wells after optical excitation, *Phys. Rev. B* **95**, 245203 (2017).
  - [5] M. Goryca, M. Koperski, P. Wojnar, T. Smoleński, T. Kazimierczuk, A. Golnik, and P. Kossacki, Coherent Precession of an Individual Spin, *Phys. Rev. Lett.* **113**, 227202 (2014).
  - [6] S. Cronenberger, D. Scalbert, D. Ferrand, H. Boukari, and J. Cibert, Atomic-like spin noise in solid-state demonstrated with manganese in cadmium telluride, *Nat. Commun.* **6**, 8121 (2015).
  - [7] C. Le Gall, L. Besombes, H. Boukari, R. Kolodka, J. Cibert, and H. Mariette, Optical Spin Orientation of a Single Manganese Atom in a Semiconductor Quantum Dot Using Quasiresonant Photoexcitation, *Phys. Rev. Lett.* **102**, 127402 (2009).
  - [8] M. Hirsch, R. Meyer, and A. Waag, Excitons as intermediate states in spin-flip Raman scattering of electrons bound to donors in Cd<sub>1-x</sub>Mn<sub>x</sub>Te epilayers, *Phys. Rev. B* **48**, 5217 (1993).
  - [9] W. Liu, Q. Lin, H. Li, K. Wu, I. Robel, J. M. Petyga, and V. I. Klimov, Mn<sup>2+</sup>-doped lead halide perovskite nanocrystals with dual-color emission controlled by halide content, *J. Am. Chem. Soc.* **138**, 14954 (2016).
  - [10] D. Rossi, D. Parobek, Y. Dong, and D. H. Son, Dynamics of exciton-Mn energy transfer in Mn-doped CsPbCl<sub>3</sub> perovskite nanocrystals, *J. Phys. Chem. C* **121**, 17143 (2017).
  - [11] Z. Chen, H. Chen, C. Zhang, L. Chen, Z. Qin, H. Sang, X. Wang, and M. Xiao, Excitation-tailored dual color emission of manganese(II)-doped perovskite nanocrystals, *Appl. Phys. Lett.* **114**, 041902 (2019).
  - [12] A. D. McCarty, A. K. Hassan, L.-C. Brunel, K. Dziatkowski, and J. K. Furdyna, Electron Paramagnetic Resonance Shift in

- $\text{II}_{1-x}\text{Mn}_x\text{VI}$  Diluted Magnetic Semiconductors in the Presence of Strong Exchange Coupling, *Phys. Rev. Lett.* **95**, 157201 (2005).
- [13] C. Kehl, G. V. Astakhov, K. V. Kavokin, Yu. G. Kusrayev, W. Ossau, G. Karczewski, T. Wojtowicz, and J. Geurts, Observation of the magnetic soft mode in (Cd, Mn)Te quantum wells using spin-flip Raman scattering, *Phys. Rev. B* **80**, 241203(R) (2009).
- [14] J. Debus, V. F. Sapega, D. Dunker, D. R. Yakovlev, D. Reuter, A. D. Wieck, and M. Bayer, Spin-flip Raman scattering of the resident electron in singly charged (In, Ga)As/GaAs quantum dot ensembles, *Phys. Rev. B* **90**, 235404 (2014).
- [15] J. Debus, D. Kudlacik, V. F. Sapega, T. S. Shamirzaev, D. R. Yakovlev, D. Reuter, A. D. Wieck, A. Waag, and M. Bayer, Basic requirements of spin-flip Raman scattering on excitonic resonances and its modulation through additional high-energy illumination in semiconductor heterostructures, *Phys. Solid State* **60**, 1611 (2018).
- [16] J. Debus, D. Dunker, V. F. Sapega, D. R. Yakovlev, G. Karczewski, T. Wojtowicz, J. Kossut, and M. Bayer, Spin-flip Raman scattering of the neutral and charged excitons confined in a CdTe/(Cd, Mg)Te quantum well, *Phys. Rev. B* **87**, 205316 (2013).
- [17] N. Samarth and J. K. Furdyna, Electron paramagnetic resonance in  $\text{Cd}_{1-x}\text{Mn}_x\text{S}$ ,  $\text{Cd}_{1-x}\text{Mn}_x\text{Se}$ , and  $\text{Cd}_{1-x}\text{Mn}_x\text{Te}$ , *Phys. Rev. B* **37**, 9227 (1988).
- [18] A. Petrou, D. L. Peterson, S. Venugopalan, R. R. Galazka, A. K. Ramdas, and S. Rodriguez, Raman scattering study of the magnetic excitations in diluted magnetic semiconductors in the presence of an external magnetic field, *Phys. Rev. B* **27**, 3471 (1983).
- [19] For  $\sigma^+$  excitation, the scattering intensities of the oppositely polarized SF lines differ by a factor of 110. This ratio is rather similar to the extinction ratio of the optical elements analyzing the polarization; thus, their imperfections lead to the SF signals in the polarization configurations other than ( $\sigma^+$ ,  $\sigma^+$ ).
- [20] D. Keller, D. R. Yakovlev, B. König, W. Ossau, T. Gruber, A. Waag, and L. W. Molenkamp, Heating of the magnetic ion system in (Zn, Mn)Se/(Zn, Be)Se semimagnetic quantum wells by means of photoexcitation, *Phys. Rev. B* **65**, 035313 (2001).
- [21] J. Debus, V. Yu. Ivanov, S. M. Ryabchenko, D. R. Yakovlev, A. A. Maksimov, Yu. G. Semenov, D. Braukmann, J. Rautert, U. Löw, M. Godlewski, A. Waag, and M. Bayer, Resonantly enhanced spin-lattice relaxation of  $\text{Mn}^{2+}$  ions in diluted magnetic (Zn, Mn)Se/(Zn, Be)Se quantum wells, *Phys. Rev. B* **93**, 195307 (2016).
- [22] The excitation energy was fixed at 2.7980 eV; thus, the resonance conditions were changed with rising magnetic field strength. Their impact is nevertheless rather weak, since the absolute change of the exciton energy amounts to 1.5 meV for increasing  $B$  from 3 to 8 T.
- [23] S. A. Crooker, J. J. Baumberg, F. Flack, N. Samarth, and D. D. Awschalom, Terahertz Spin Precession and Coherent Transfer of Angular Momenta in Magnetic Quantum Wells, *Phys. Rev. Lett.* **77**, 2814 (1996).
- [24] J. Stühler, G. Schaack, M. Dahl, A. Waag, G. Landwehr, K. V. Kavokin, and I. A. Merkulov, Multiple  $\text{Mn}^{2+}$ -Spin-Flip Raman Scattering at High Fields via Magnetic Polaron States in Semimagnetic Quantum Wells, *Phys. Rev. Lett.* **74**, 2567 (1995).
- [25] K. V. Kavokin and I. A. Merkulov, Multispin Raman paramagnetic resonance: Quantum dynamics of classically large angular momenta, *Phys. Rev. B* **55**, R7371(R) (1997).
- [26] L. C. Smith, J. J. Davies, D. Wolverson, M. Lentze, J. Geurts, T. Wojtowicz, and G. Karczewski, Dependence of multiple spin-flip Raman scattering in quantum wells on the magnetic field direction, *Phys. Rev. B* **77**, 115341 (2008).
- [27] A. V. Koudinov, Yu. G. Kusrayev, B. P. Zakharchenya, D. Wolverson, J. J. Davies, T. Wojtowicz, G. Karczewski, and J. Kossut, Spin-flip Raman scattering in semi-magnetic quantum wells with in-plane anisotropy: Analysis of the intermediate states, *Phys. Rev. B* **67**, 115304 (2003).
- [28] F. Teppe, M. Vladimirova, D. Scalbert, T. Wojtowicz, and J. Kossut, Optically induced instability of spin precession in magnetic quantum wells, *Phys. Rev. B* **67**, 033304 (2003).
- [29] A. Kavokin and G. Malpuech, Formation of spin domains in semimagnetic quantum wells: Theory, *Phys. Rev. B* **68**, 205206 (2003).
- [30] D. J. English, P. G. Lagoudakis, R. T. Harley, P. S. Eldridge, J. Hübner, and M. Oestreich, Strain-induced spin relaxation anisotropy in symmetric (001)-oriented GaAs quantum wells, *Phys. Rev. B* **84**, 155323 (2011).
- [31] A. Abragam, *The Principles of Nuclear Magnetism* (Oxford University Press, Oxford, 1983), Chap. VII, p. 233.
- [32] C. P. Slichter, *Principles of Magnetic Resonance* (Springer-Verlag, Berlin, Heidelberg, 1978), Chap. 10, p. 496.
- [33] K. V. Kavokin and I. A. Merkulov, Carrier relaxation at magnetic ion pairs in semimagnetic quantum wells, *Phys. Solid State* **36**, 1480 (1994).
- [34] G. Winterling and E. Koteles, Resonant Brillouin scattering near the A exciton in CdS, *Solid State Commun.* **23**, 95 (1977).
- [35] A. Stasch, Raman scattering from spin-flip and magnon excitations in magnetic semiconductors, *J. Phys. C: Solid State Phys.* **16**, 4057 (1983).
- [36] M. K. Kneip, D. R. Yakovlev, M. Bayer, A. A. Maksimov, I. I. Tartakovskii, D. Keller, W. Ossau, L. W. Molenkamp, A. Waag, Spin-lattice relaxation of Mn ions in ZnMnSe/ZnBeSe quantum wells measured under pulsed photoexcitation, *Phys. Rev. B* **73**, 045305 (2006).
- [37] L. Besombes, H. Boukari, C. Le Gall, A. Brunetti, C. L. Cao, S. Jamet, and B. Varghese, Optical control of the spin of a magnetic atom in a semiconductor quantum dot, *Nanophotonics* **4**, 75 (2015).
- [38] *Solid State Physics*, edited by F. Seitz and D. Turnbull (Academic Press, London, 1963), Vol. 14, p. 204.